ELSEVIER

Polymer 40 (1999) 3979–3988

polymer

The effect of DMPA units on ionic conductivity of PEG–DMPA–IPDI waterborne polyurethane as single-ion electrolytes

Ten-Chin Wen[a,*], Yeong-Jyh Wang[a], Tsung-Tien Cheng[a], Chien-Hsin Yang[b]

[a]*Department of Chemical Engineering, National Cheng Kung University, Tainan 701, Taiwan, ROC*
[b]*Department of Environmental and Chemical Engineering, Kung Shan Institute of Technology, Tainan 710, Taiwan, ROC*

Received 28 April 1998; received in revised form 18 August 1998; accepted 28 August 1998

Abstract

The waterborne polyurethane (WPU) dispersions synthesized from poly(ethylene glycol) (PEG), dimethylol propionic acid (DMPA), and isophorone diisocyanate (IPDI) with various DMPA contents were prepared from our modified acetone process. Differential scanning calorimeter (DSC), Fourier transform infrared spectroscopy (FT-i.r.), and wide-angle X-ray diffraction spectroscopy (WAXD) were utilized to characterize WPU films for the behavior of their crystallinity and H-bonding. Alternating current (AC) impedance experiments were performed to determine the ionic conductivities of WPU films and their corresponding gel electrolytes. One of the investigated WPU gel electrolytes exhibits an ionic conductivity as high as $\sim 10^{-5}$ S/cm at room temperature.

Keywords: Poly(ethylene glycol) (PEG); Dimethylol propionic acid (DMPA); Waterborne polyurethane

1. Introduction

Since poly(ethylene oxide) (PEO) electrolytes were reported by Wright et al. [1, 2], solid polymer electrolytes (SPE) have attracted many studies on lithium ion polymer batteries. Most of the researchers have concentrated on designing novel polymer materials possessing high ionic conductivity, good mechanical properties as well as thermal stability for technological applications [3–5].

Among the interesting polymer electrolytes that were developed, polyether-based electrolyte showed features such as good adherence to electrodes and the ability to solvate many inorganic salts. Ionic conductive polymers such as complexes of PEO and lithium salts, which showed high ionic conductivity of 10^{-4} to 10^{-3} S/cm at high temperature were characterized by a bi-ion transport mechanism [6–9]. The defect of these materials is the significant decrease in ionic conductivity using direct current polarization. Therefore, an ionic conductive polymer with single-ion transport mechanism is required for a number of applications. Generally, the ionic conductivity of single-ion transport materials is lower than that of the bi-ion transport materials. Several ionic conductive polymers have been characterized by a single-ion transport mechanism [10]. Most of them are polyblends of polymer and polyether or copolymers synthesized from polymers with low molecular weight of polyether. It should be noted that polyblend electrolytes show poor mechanical properties, and that copolymer electrolytes show low conductivity [11].

Although there is no common agreement on the exact mechanism of ionic transport in polymer-based electrolytes, it is conceivable that significant motion exists only in the amorphous phase of polymers while nonconducting in the crystalline phase [12]. Thus, in order to design an excellent polymer electrolyte, the degree of crystallinity of the polymer should be lowered, while adequate mechanical properties should be maintained for practical applications. Ease of film fabrication is another necessary consideration. However, pure PEO is a semicrystalline polymer, possessing both amorphous and crystalline phases at room temperature. Hence, considerable ionic conductivity in PEO-based polymers can only be obtained at high temperature [13]. From the above fundamental knowledge, in designing a novel polymer of similar PEO structure, it is reasonable that a PEG reacted with diisocyanate to form a PEG-based polyurethane (PU), because PU polymer belongs to a elastomer possessing high tensile strength, elasticity as well as low crystallinity. In general, PUs comprise linear copolymers with soft and hard segment structure. Basically, this material consists of a relatively flexible component, the so-called soft segment, and a relatively polar and stiff component known as the hard segment. The

* Corresponding author. Tel.: +886-6-2757575 Ext. 62656; fax: +886-6-2344496.
E-mail address: tcwen@mail.ncku.edu.tw (Ten-Chin Wen)

0032-3861/99/$ - see front matter
PII: S0032-3861(98)00625-9

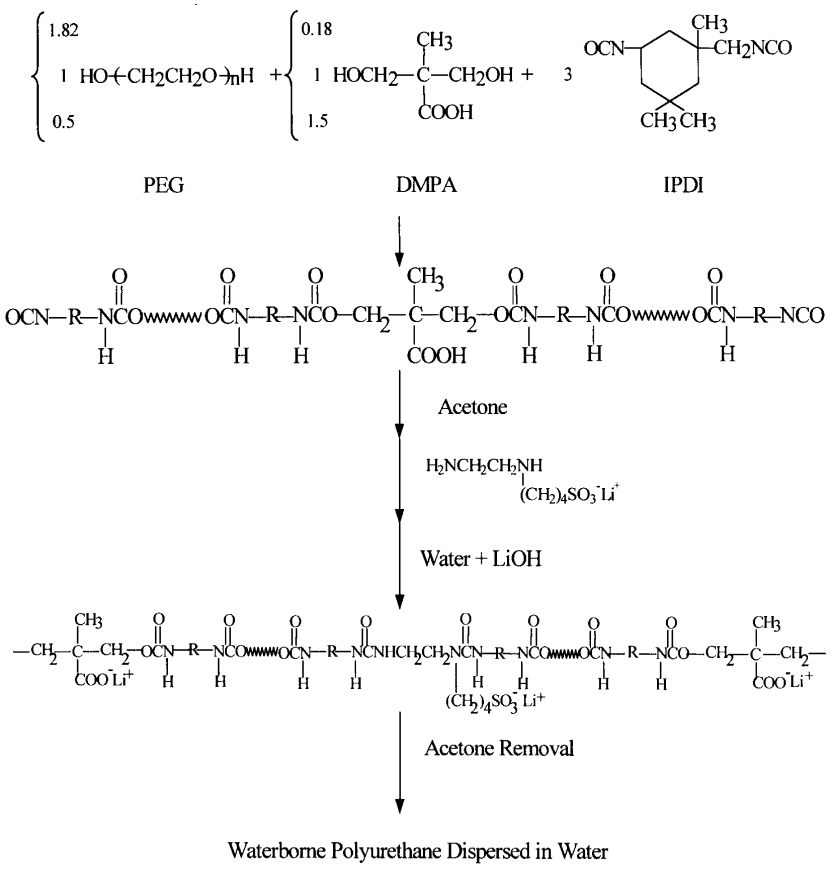

Where

wwwww = $+CH_2CH_2O+_n$

-R- =

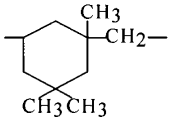

Scheme 1. The preparation process for WPU dispersion.

soft segment is poly(glycol), and the hard segments consist of diisocyanate and chain extenders, e.g. diols and diamines. The hard segment provides both physical crosslink sites and filler-like reinforcement to soft segment matrix. The properties of PU are significantly influenced by the ratio of hard and soft block components and the average block lengths employed. In polyurethane, the fraction of hard–hard segment H-bonding (NH···O=C) was used as a measure of the extent of phase separation, and hard–soft segment H-bonding (NH···O) represents the extent of phase mixing between hard and soft segments [14–18].

Polymer matrix is usually mixed with a small polar solvent (plasticizer) such as ethylene carbonate (EC) or propylene carbonate (PC), which are used to improve conductivity [19]. This category of polymer electrolyte containing polar solvent is called gel-type electrolyte. In this case, the solvent plays the role of the ion supporting carrier and the plasticizer of polymer matrix, enhancing the mobility of ions and the flexibility of polymer electrolyte.

More recently in our laboratory, we have successfully developed a series of WPU materials in which the mixture of PEG and DMPA were polymerized with IPDI via urethane linkages to yield an aqueous dispersion of PU ionomer [20, 21]. In the present work, samples of PEG-based WPU polymer electrolytes with various DMPA/PEG ratios were characterized by Fourier transform infrared spectroscopy (FT-i.r.), wide-angle X-ray diffraction spectroscopy (WAXD) and differential scanning calorimetry (DSC). The ionic conductivities of all samples were obtained by running AC impedance experiments.

Table 1
Molecular mass distribution of PU prepolymers

Sample	[DMPA]/[PEG]	M_n	M_w	M_w/M_n
A	0.1	8220	28 220	3.43
B	1	10 360	25 830	2.49
C	3	6800	12 410	1.82

2. Experimental

2.1. Materials

PEG ($M_w = 2000$, Showa), used as the soft segment, was dried at 75°C in a vacuum oven for 72 h. IPDI (Lancaster) and DMPA (Aldrich), used as the hard segment were vacuum dried at 80°C for 24 hrs. PC (Aldrich) were distilled at low pressure and stored over 3 Å molecular sieves before use. Acetone (Tedia) and *N*-methyl-2-pyrrolidinone (NMP) (Aldrich) were immersed in 4 Å molecular sieves for more than 1 week before use. Di-*n*-butyltin(IV)dilaurate (DBTDL) (Wako), ethylenediamine (EDA) (Merck), and butane sultone (BS) (Aldrich) were used without further treatment.

2.2. Preparation of WPU dispersion

The WPU dispersion was prepared through our modified acetone process with NCO/OH = 1.5 [3]. The process of synthesis is shown in Scheme 1. The solution of PEG and DMPA/NMP was added to the reactor and heated to 50°C. IPDI and catalyst DBTDL were then added to the mixture and reacted at 85°C under nitrogen atmosphere for 6 h. To the final NCO-terminated PU prepolymer was added a suitable amount of acetone. Typical molecular masses of PU prepolymers are listed in Table 1. Lithium hydroxide (LiOH), as neutralizing agent, and an ethylenediamine-based chain extender bearing sulfonate groups in aqueous solution (see Refs. [3, 21], neutralized with LiOH) were added immediately to the freshly prepared NCO-terminated PU prepolymer solution. The resulting mixture was then heated at phase-inversion temperature of 50°C, yielding PU anionmers in acetone. The stoichiometric ratio of LiOH to COOH was 1.0. Doubly distilled water was added to neutralizing PU anionmer solutions at agitation rate and water addition rate of 200 rev/min and 2.0 mL/min, respectively. An aqueous dispersion of about 30 wt% solids was obtained upon removal of acetone by rotary vacuum evaporation.

Table 2
Characteristics of the film derived from PEG-based waterborne polyurethane

Sample	[DMPA]/[PEG]	SSC[a] in WPU (mol%)	$[Li^+]/[EO^b]$	T_g (°C)	T_m (°C)
A	0.1	36.4	0.006	− 54.5	32.1
B	1	20	0.032	− 50.3	22.7
C	3	10	0.091	− 50.2	–

[a] SSC, soft segment content.
[b] EO, concentration of ethylene oxide units on WPU.

2.3. Molecular weight

The MWD and average molecular weight of the PU prepolymer were determined by GPC (Shimatsu R-7A data module; LC-10AS pump). The separation columns were two linear columns in series. The flow rate for THF was 1 mL/min at 40°C using polystyrene standards.

2.4. Sample preparation and measurement

The films from the solvent evaporation method were obtained by casting the WPU dispersion solution on a Teflon disk, followed by drying at 45°C for 2 days. The films were then removed to a glove box for further drying. Before all tests on these films, the water content of the films was determined to be around 10 ppm using a Karl Fisher moisture titrator (MKC-210, Kyoto Electronics, Japan) for the film extracted solvent (acetone). The characteristics of the film derived from PEG-based WPU are listed in Table 2.

2.5. AC impedance

Impedance analysis of the polymer electrolyte was performed using a CMS300 EIS system (Gamry Instrument, USA) with SR810 DSP lock-in amplifier (Standard Research System, USA) under an oscillation potential of 10 mV from 100 kHz to 0.1 Hz. The WPU films or their corresponding gel electrolytes were sandwiched by two stainless steel (SS304) blocking electrodes for conductivity tests.

2.6. DSC measurement

Thermal analysis of WPU films was carried out using Du Pont system DSC (Du Pont 910, USA) with a temperature range from − 100°C to 100°C at a heating rate 10°C/min under nitrogen purging.

2.7. FT-i.r. measurement

The samples for infrared analysis were prepared by casting 1% (w/v) WPU solution, NMP as solvent, directly on KBr pellets and drying at 80°C in a vacuum oven for 24 h. Infrared spectra were obtained with a Fourier Transform IR spectrophotometer (Nicolet FTIR-550) and recorded by averaging 64 scans at a resolution of 4 cm^{-1}.

2.8. WAXD

WAXD was carried out on a Rigaku D/MAX-IIIV diffractometer using CuKα radiation and the 2θ scanning rate was 4°/min with a range from 40° to 4°.

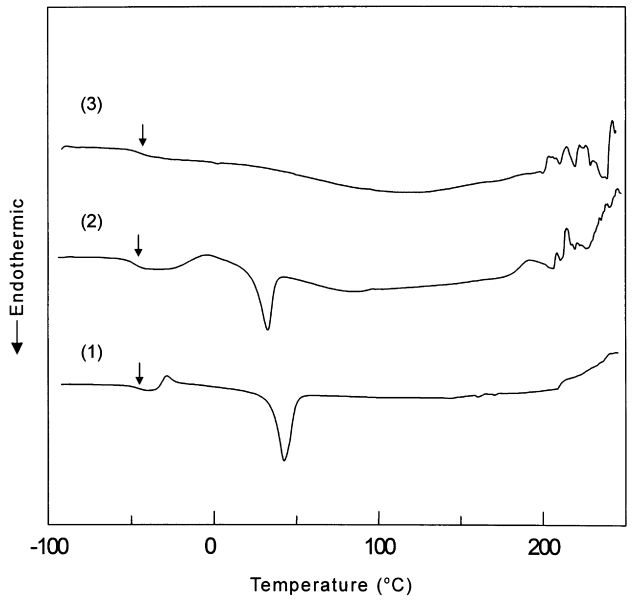

Fig. 1. DSC thermograms at the heating rate of 10°C/min for WPU films with various DMPA/PEG ratios: (1) sample A; (2) sample B; (3) sample C.

3. Results and discussion

3.1. DSC

Fig. 1 shows the DSC thermograms of three investigated polymer samples, indicating crystallinity for samples A and B, and but not for sample C. For these investigated polymers, a soft-segment T_g of -52.5 to -50.2°C was observed, which is substantially lower than that of pure PEG (about -46°C) [22]. Meanwhile, a soft-segment T_m of 32.1 to 22.7°C was observed, which is substantially lower than that pure PEG (about 52°C). These results indicate that the polymers have a certain degree of hard- and soft-segment mixing. The soft-segment T_g decreases in the order: sample A > sample B > sample C. This corresponds to phase separation in the order: sample A > sample B > sample C. The soft-segment T_m values of samples A and B are observed in the range from 32.1 to 22.7°C; however, the soft-segment T_m of sample C is not detected. According to Cooper et al. [23], three characteristic endotherm transitions observed at 60–80°C, 120–190°C and 200°C correspond respectively to the short range, long range and microcrystalline ordering of hard-segment domains. Therefore, the observed hard-segment T_g of sample C may be attributed to phase-segregated structures of the shorter hard-segment unit (DMPA). On the other hand, the soft-segment T_m decreases in the order: sample A > sample B > sample C. This result suggests that a polymer chain with higher DMPA content exhibits a lower degree of crystallinity. One possible explanation for this is that the degree of mixing of hard and soft segments increases with the addition of DMPA. In addition, note that devitrification exists in samples A and B, occurring at -33.6°C and -6.3°C,

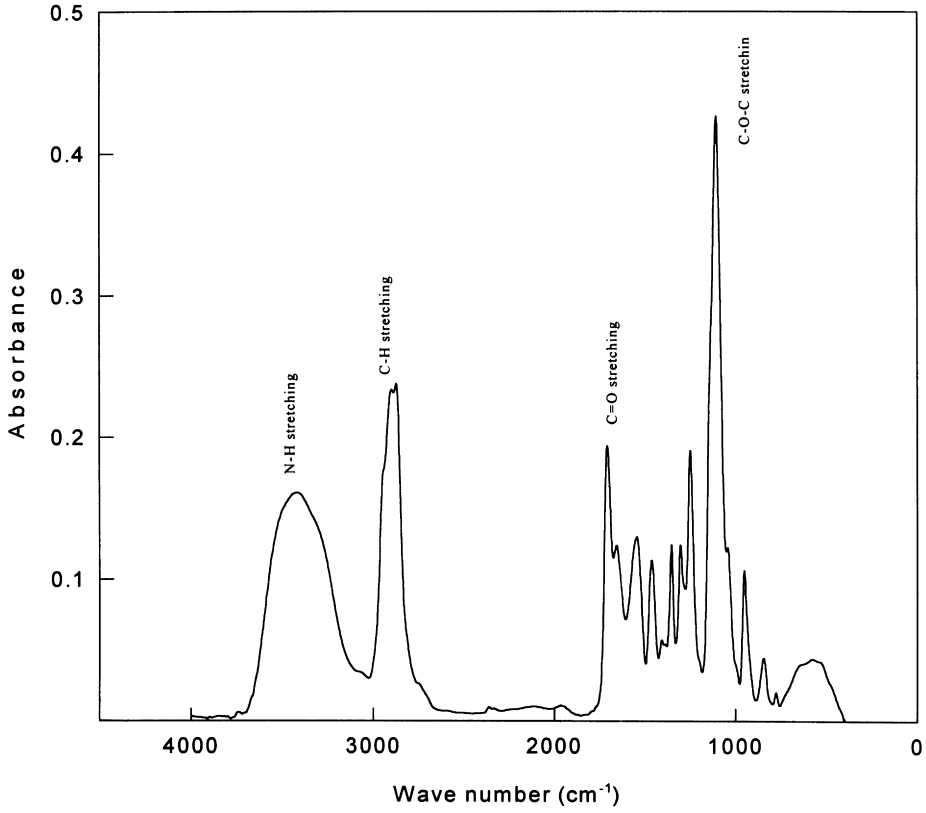

Fig. 2. Typical FT-i.r. spectrum of PEG-based waterborne polyurethane (sample B).

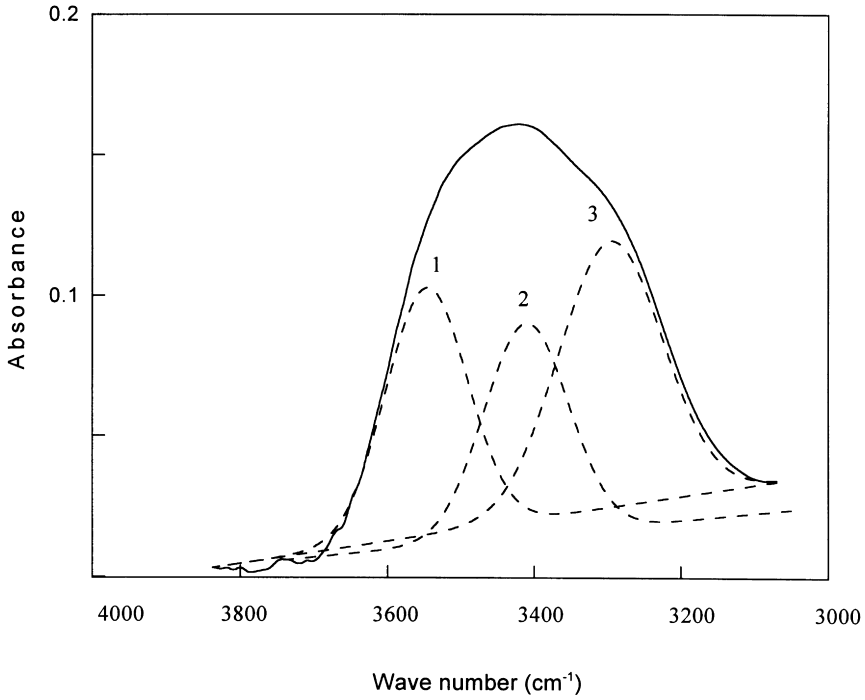

Fig. 3. FT-i.r. spectrum (solid line) and deconvolution curves (dashed line) of WPU film (sample B) in N–H stretching region.

respectively. Devitrification appears as an exotherm and is followed by an endotherm at a higher temperature that corresponds to the melting of these crystals (samples A and B). This implies that there should exist a nucleating phase of crystal structure in low DMPA-containing polymers during temperature scanning. After nucleation, crystal growth rates are small because the glass phase is heated to a higher temperature, at which crystal growth occurs on the surface of the existing nuclei. Because there is a large number of nuclei present, distributed throughout the bulk of the glass, each can grow by only a small amount until it impinges on neighboring nuclei. Hence, the final crystal size in this case should be small.

3.2. FT-i.r. spectroscopy

In this study, adjustment of the polymer ionization level was achieved by varying DMPA/PEG ratios in the polymer chain, i.e. when the DMPA content is increased more Li^+ is required to neutralize the anion (–COOH) in the DMPA unit. In order to identify the structure of these WPU, FT-i.r. was employed and a typical spectrum is shown in Fig. 2. Four main regions are presented.

1. 3300 ~ 3600 cm^{-1} N–H stretching, a broad absorption band of the N–H region was observed.
2. 1600 ~ 1750 cm^{-1} C=O stretching, the carbonyl stretching absorption band was observed to be composed of two peaks. The higher frequency at around 1700 cm^{-1} was assigned to free (i.e. not H-bonded) carbonyl stretching while the peak at around 1660 cm^{-1} was attributed to H-bonded carbonyl stretching.
3. 1500 ~ 1600 cm^{-1} COO^-Li^+ stretching, characteristic of the pendant group from the hard-segment of DMPA.
4. 1000 ~ 1150 cm^{-1} C–O–C stretching, the ether oxygen of the soft-segment.

FT-i.r. spectra have demonstrated H-bonding in PU [18]; the strength of the H-bonding was measured by frequency shifts to values lower than those observed when these groups are free. The N–H group could form hard–hard segment H-bonding with the carbonyl oxygen and hard–soft segment H-bonding with the ether oxygen. In general, the strength of hard–hard segment H-bonding is stronger than that of hard–soft segment H-bonding [11]. Deconvolution of the N–H stretching region was done and the best fits were obtained using a Gaussian–Lorentzian sum as seen in Fig. 3. It indicates that the higher frequency of the deconvoluted peak (peak 1) is assigned 'free' N–H stretching (about 3550 cm^{-1}), lower frequency (peak 3) is assigned

Table 3
Frequency shifts of H-bonded N–H stretching with respect to free N–H stretching

Sample	Frequency shift (cm^{-1})	
	H–H H-bonded N–H stretching[a]	H–S H-bonded N–H stretching[b]
A	262	125
B	251	119
C	234	117

[a] Hard–hard segment H-bonded N–H stretching.
[b] Hard–soft segment H-bonded N–H stretching.

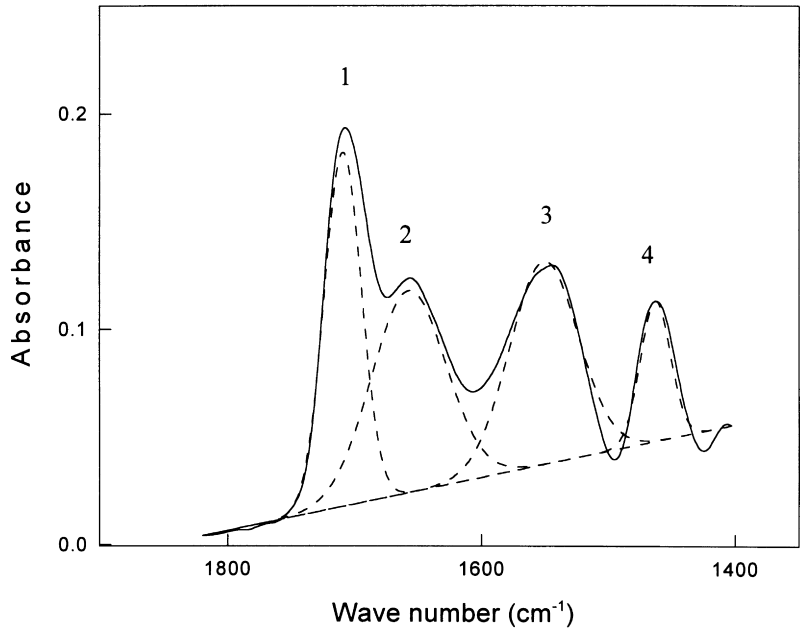

Fig. 4. FT-i.r. spectrum (solid line) and deconvolution curves (dashed line) of WPU film (sample B) in carbonyl stretching region.

N–H stretching affected by hard–hard segment H-bonding (about 3300 cm^{-1}), and the central peak (peak 2) is N–H stretching affected by hard–soft segment H-bonding (about 3430 cm^{-1}). The frequency shift of H-bonded N–H stretching represents the strength of H-boning in polyurethane [17]. The results are listed in Table 3, revealing that the H-bonding stretching of both hard–hard and hard–soft segments is in the order: sample A > sample B > sample C, and that a higher DMPA content in the polymer would reduce the stretching of H-bonding. In polyurethane, urethane groups would form hard–hard segment H-bonding with the carbonyls of urethane, urea and carboxylic groups.

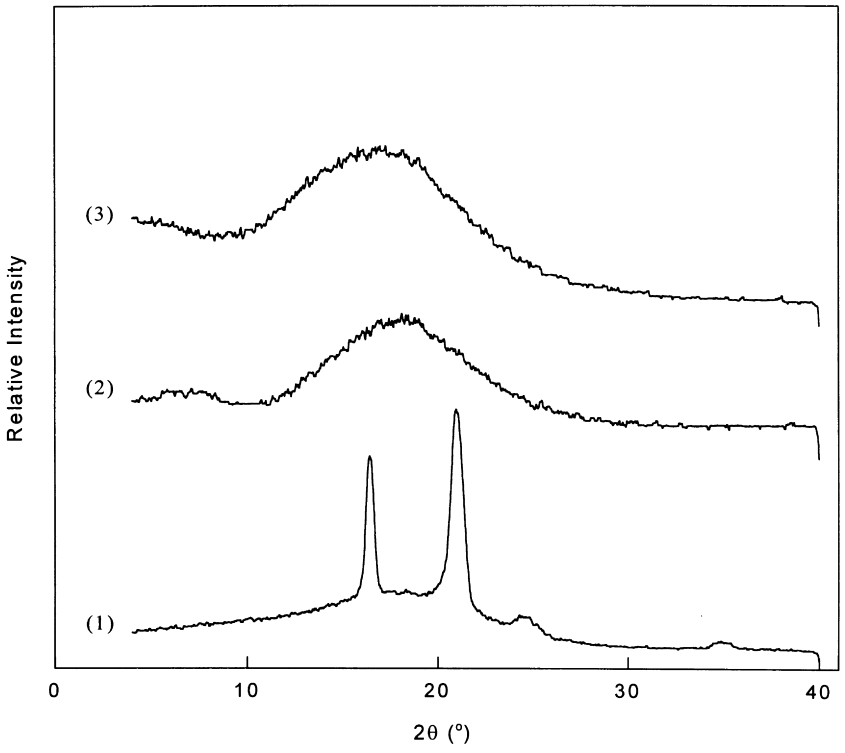

Fig. 5. WAXD spectra at a scan rate of 4°/min for WPU films with various DMPA/PEG ratios: (1) sample A; (2) sample B; (3) sample C.

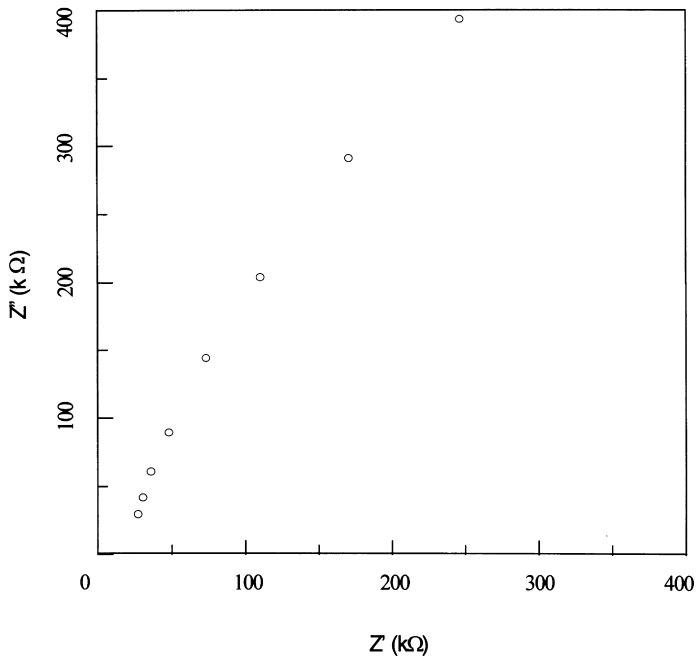

Fig. 6. Cole–Cole plot of SS/WPU film (sample B)/SS at 25°C; 150 μm thick and 0.785 cm^2 area for the film. Impedance frequency from 100 kHz to 100 Hz.

Thus, these results reflect that the H-bonding between urethane and urethane or urea is stronger than that between urethane and carboxylic groups.

The stronger hard–hard segment H-bonding acts as physical cross-links leading to difficult segmental motion of the polymer chain, which results in a more significant phase separation between hard and soft segments. This is corroborated by the DSC results with T_m in the order: sample A > sample B > sample C. In our WPU samples, the NCO/OH ratio (1.5) was kept constant. Because the soft segment content (SSC; i.e., PEG2000) in WPU decreases with increasing DMPA content, the strength of hard–soft segment H-bonding decreases with decreasing SSC content. Thus, the strength of hard–soft segment H-bonding is in the order: sample A > sample B > sample C.

Fig. 4 shows the i.r. spectra of the carbonyl stretching region for the WPU of sample B. The band centered at around 1710 ± 2 cm^{-1} (peak 1) is attributed to the stretch of free urethane carbonyl groups, while the band at 1658 ± 4 cm^{-1} (peak 2) is assigned to H-bonding urethane carbonyl groups. The latter corresponds to H-bonding in disordered regions, which comes from the urethane linkage of interfacial regions or 'dissolved' in the soft phase. For the stronger H-bonding in ordered or crystalline regions, the stretching absorbance occurs at a lower frequency of about 1550 cm^{-1} (peak 3). This frequency shift of the urea carbonyl band of WPUs from 1555 cm^{-1} (sample C) to 1540 cm^{-1} (sample A) can be attributed to some soft segments apparently dissolved in the hard-segment domains. Thus, three samples in this study show dissolved soft segments dispersed in the hard-segment domains. It provided evidence that the investigated polymers are in a mixed state of hard–soft phases. The band centered at 1470 cm^{-1} (peak 4) is assigned to the stretch of H-bonded carboxylic carbonyl groups from DMPA units.

3.3. WAXD

X-ray diffraction patterns for these WPUs are shown in Fig. 5. The broad scattering halos between 10° and 30° of 2θ are present in all samples, but sample A with higher SSC shows sharp and clear diffraction peaks at 16.4° and 21° which come from orderly arrangement of ethylene oxide group of soft segment. Yen et al. [16] suggested that the PEG chain would begin to fold on itself and form segment–segment interactions when the molecular weight of the PEG is above 1200. Additionally, two small peaks for sample A are observed at 24.3° and 35.5°, resulting from the nonpolarized portion (IPDI–PEG–IPDI) of WPU. It is obvious that sample A is a semi-crystalline ionomer and samples B and C are amorphous ionomers at room temperature as indicated by the DSC results. Owing to the semi-crystalline behavior of sample A, the broad halo region implies that the amorphous region of sample A is smaller than those of samples B and C. As the DMPA content increased in WPU, the crystalline structure collapses due to the random arrangement of the polymer chain (see samples B and C).

3.4. Ionic conductive properties

Since samples A, B, and C possess different lithium ion contents, it is interesting to investigate the ionic conducting behavior of these samples. Thus, AC impedance was performed to determine the conductivity (σ) of these films. The result was plotted as a Cole–Cole plot to show

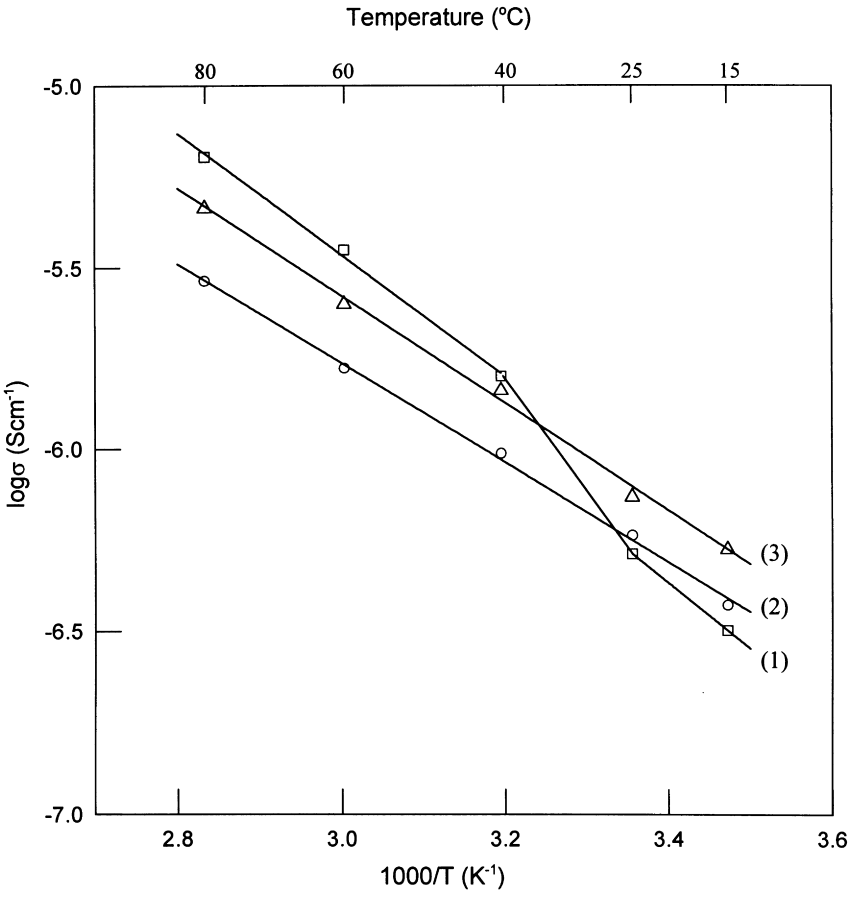

Fig. 7. Arrhenius plots of conductivity for WPU films with various DMPA/PEG ratios: (1) sample A; (2) sample B; (3) sample C.

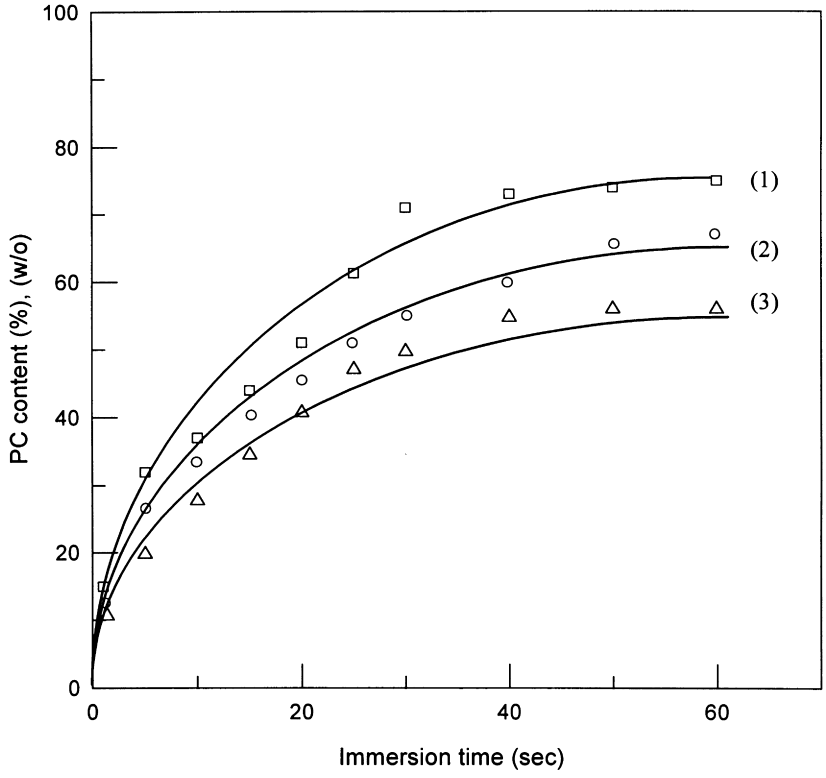

Fig. 8. Swelling rate for WPU films with various DMPA/PEG ratios: (1) sample A; (2) sample B; (3) sample C.

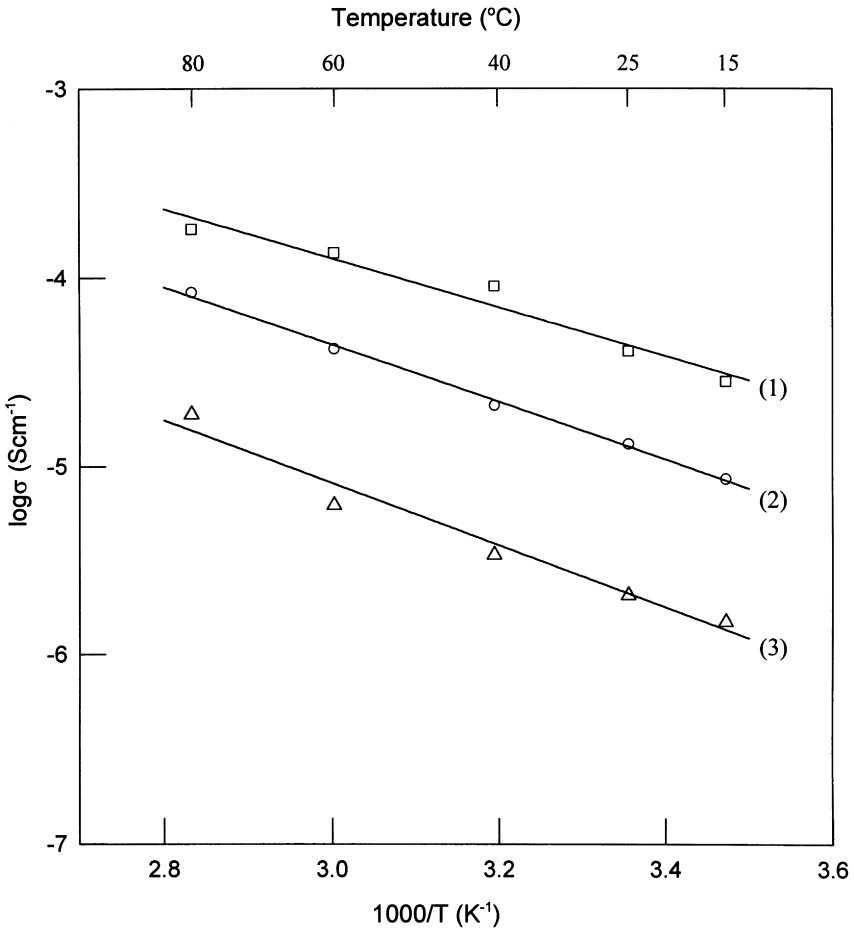

Fig. 9. Arrhenius plots of conductivity for various WPU gel electrolytes (containing 50 wt% PC): (1) sample A; (2) sample B; (3) sample C.

the real/image parts of impedance at various frequencies. A typical Cole–Cole plot of WPU film sandwiched between stainless steel electrodes is shown in Fig. 6. The profile shows a straight line in which the impedance (the distance from the experimental point to the original) decreases with increasing frequency. It indicates that the interfacial impedance decreases with increasing frequency, which is attributed to double layer formation and charge transfer reaction. At a frequency approaching 100 kHz, the line closes to the real axis, indicating that the impedance approaches pure resistance. In this case, the interfacial impedance is negligible and the bulk resistance (R_b) is obtained. The conductivity of WPU film can be determined by letting $\sigma = (1/R_b)(l/A)$, where l and A represent film thickness and surface area of the film, respectively. Fig. 7 shows the Arrhenius plots of ionic conductivity for samples A, B, and C, comprising two straight lines for samples B (line 2) and C (line 3) but a two-segmental line (line 1) for sample A. It indicates that the conductivities of these three samples obey the Arrhenius law while sample A possesses a transition zone between 25 and 40°C. This transition zone might be due to the fact that this polymer has T_m between 25 and 40°C (see DSC results), as the migration of lithium ion should be easier in melted polymer than in the crystalline form. In contrast, sample B shows an endothermic peak for DSC results without a transition zone for conductivity. It is conceivable that sample B was amorphous at room temperature but was crystallized as it was cooled to -15°C before running the DSC experiment. Thus, samples B and C possess similar amorphous structures, which provide similar environments for ion conduction, resulting in nearly the same activation energy. In this case, sample C possesses more lithium ion than sample B, leading to a higher conductivity. Sample A possesses the lowest conductivity at temperatures lower than 25°C, which might be attributed to the lowest lithium ion content. At temperatures above 40°C, owing to the crystalline region of sample A being melted, lithium ion could migrate easily in the soft phase without the interference of electronegative groups, e.g. COO^-, urethane/urea groups, resulting in sample A showing higher conductivity than the other two samples.

In order to improve the conductivity, samples A, B, and C were impregnated with PC to form gel-type electrolytes. The swollen weight was measured versus various immersion times and the results were plotted in Fig. 8. It reveals lines 1, 2, and 3 as saturated curves for samples A, B, and C, respectively. The swelling rate may be obtained from the slope of the curves and saturated weight after 1 min can be

found. Note that the swelling rate and the saturated swollen weight increase with decreasing DMPA/PEG ratio, indicating that the decrease in DMPA/PEG is helpful in the absorption of PC. This result reflects that the shorter hard segment (DMPA) in WPU yields the more urethane groups. These groups form hydrogen bonding hard phase to retard PC absorption. Also note that PC is mainly absorbed in soft phase of PEG. Thus, the devitrification structure (DSC results), which come from PEG ethylene oxide, is dominant for PC absorption.

In order to understand the effects of DMPA/PEG on the conductivity of WPU gel electrolytes, the swollen weight of PC in samples A, B, and C was controlled at 50 wt% and consequently AC impedance was performed. Arrhenius plots of conductivity for these gel electrolytes are shown in Fig. 9. All are straight lines, meaning that the conductivity of these films also obeys Arrhenius law. Note that there is no transition zone in curve 1 (sample A). It could be deduced that the lithium ion is completely solvated by PC solvent, resulting in the collapse of crystalline structure in sample A. Hence, the ion-conduction behavior of the gel-film (containing solvent) is quite different from that of the solvent-free film. Also note that the conductivity decreases with increasing DMPA content, indicating that the increase in the pendant group would not increase the conductivity. In our opinion, the pendant group from DMPA would attract Li^+ and block the motion of Li^+ in gel electrolyte, resulting in a decrease of conductivity. In this case, the room temperature conductivity of sample A was increased to about 5×10^{-5} S/cm, revealing that the WPU film with a suitable modification is possibly used as a single-ion electrolyte.

4. Conclusion

The degree of crystallinity and the strength of H-bonding decreases with increasing DMPA content in WPU. The addition of DMPA in WPU provides lithium ion for conduction but also gives pendant groups for blocking ion migration. The conductivity of WPU gel electrolytes which are prepared by adding 50% (w/o) PC in WPU films increases with decreasing DMPA content. Thus, a WPU gel electrolyte with a DMPA/PEG ratio of 0.1 exhibits an ionic conductivity as high as $\sim 10^{-5}$ S/cm at room temperature. This implies that this type of WPU gel electrolyte has potential for use as a single-ion electrolyte.

Acknowledgements

The financial support of this work by the National Science Council of the Republic of China under contract NSC 87-2214-E-006-026, is gratefully acknowledged.

References

[1] Wright V. Br Polym 1975;7:319.
[2] Armand MB. Solid State Ionics 1983;9/10:745.
[3] Yang CH, Lin SM, Wen TC. Polym Eng Sci 1995;35:722.
[4] Murata K. Electrochim Acta 1995;40:2177.
[5] Fauteux D, Massucco A, Mclin M, van Buren M, Shi J. Electrochim Acta 1995;40:2185.
[6] Barthel J, Buestrich R, Carl E, Gores HJ. J Electrochem Soc 1996;143:3565.
[7] Lee HS, Yang XQ, McBreen J, Xu ZS, Skotheim TA, Okamoto Y. J Electrochem Soc 1994;141:886.
[8] Shodai T, Owens BB, Ohtsuka H, Yamaki J. J Electrochem Soc 1994;141:2978.
[9] Ramanujachary KV, Tong X, Lu Y, Kohn J, Greenblatt M. J Appl Polym Sci 1997;63:1449.
[10] Xu HS, Yang CZ. J Polym Sci: Part B: Polym Phys 1995;33:745.
[11] Zorans Petrovic. J Polym Sci: Part B: Polym Phys 1989;27:545.
[12] Berthier C, Gorecki W, Minier M, Armand MB, Chabagno JM, Rigand P. Solid State Ionic 1983;11:91.
[13] Farrington GC, Linford RG. In: MacCallum JR, Vincent CA, editors. Polymer electrolyte reviews 2. London: Elsevier, 1989:255.
[14] Martin DJ, Meijs GF, Renwick GM, Mccarthy SJ, Gunatillake PA. J Appl Polym Sci 1996;62:1377.
[15] Martin DJ, Meijs GF, Renwick GM, Mccarthy SJ, Gunatillake PA. J Appl Polym Sci 1996;60:557.
[16] Yen MS, Kuo SC. J Appl Polym Sci 1996;61:1639.
[17] Teo LS, Chen CY, Kuo JF. Macromolecules 1997;30:1793.
[18] Van Heumen JD, Stevens JR. Macromolecules 1995;28:4268.
[19] Huq R, Koksbang R, Tonder PE, Farrington GC. Electrochim Acta 1992;37:1681.
[20] Cheng YT, Wen TC. Solid State Ionic 1998;107:161.
[21] Yang CH, Li YJ, Wen TC. Ind Eng Chem Res 1997;36:1614.
[22] Brandrup J, Immergut EH. Polymer handbook, 3rd ed. New York: Wiley, 1989.
[23] Wang CB, Cooper SL. Macromolecules 1983;16:775.